Accurate Determination of Vertical Air Velocities in Rain by Doppler-Radar

Klaassen, Wim

Published in:
Journal of Climate and Applied Meteorology

DOI:
10.1175/1520-0450(1983)022<1788:ADOVAV>2.0.CO;2

Publication date:
1983

Accurate Determination of Vertical Air Velocities in Rain by Doppler-Radar

WIM KLAASSEN

IMOU, Rijksuniversiteit Utrecht, Utrecht 2506 The Netherlands

(Manuscript received 17 August 1982, in final form 5 April 1983)

ABSTRACT

Vertical air velocity in rain is calculated from the minima in the reflectivity profile of the Doppler velocity spectra between succeeding range cells. The reflectivity minimum is converted to air velocity, assuming a negative exponential dropsize distribution. The scatter in the observed reflectivity minima can be lowered considerably by representing the reflectivity profile around the minima with a best-fit second order polynomial. A statistical method is developed to express the observed scatter in true fluctuations of the air velocity and a measurement error. In this way the accuracy of the method could be calculated and compared to other methods.

Experimental verification has been made during a steady rain with a vertically directed FM–CW Doppler radar. This type of radar is very suitable for this kind of measurements because of its high sensitivity and range resolution. High quality pulse Doppler radars might also be used. Accuracies in the mean vertical air velocity of a few cm s^{-1} have been obtained. However, just below the bright band larger errors were found, due to deviations from the assumed dropsize distribution by some large, partly melted snowflakes. Turbulent fluctuations of the vertical air velocity in a space volume of $60 \times 20 \times 20$ m and a sampling time of 3 s were determined with a rms accuracy of 0.11 m s^{-1}. Even in the stratiform rain this measurement error appeared much smaller than the scatter in the true air velocity and the errors that should be made by estimating the air velocity from the mean fall velocity. It is expected that these differences will be even more pronounced in turbulent precipitation.

1. Introduction

Doppler–radar at vertical incidence may be used to measure the fall velocity of rain. As the fall velocity of raindrops is a function of drop size, the drop-size distribution can also be determined from accurate velocity observations. Atlas *et al.* (1973) found that the fall velocity has to be determined with an accuracy better than ± 0.25 m s^{-1} to calculate the number of raindrops of given size between 0.5 and 4 mm diameter to within a factor of 2. The main problem is that the fall velocity has to be determined relative to the surrounding air. Therefore accurate measurements of turbulent air velocity have to be made simultaneously.

As fall velocity is increasing with rain drop diameter, air velocity can be calculated from the fall velocity of the smallest drops. The smallest drops are also marked by their poor reflectivity in the Doppler velocity spectra. Therefore air velocity can be determined from the minima in the Doppler velocity spectra. Compared to the Lower Boundary Technique (Atlas *et al.*, 1973) this method is less sensitive to instrumental noise and the minimum reflectivity velocity is easy to determine, but the results are strongly dependent on the adjustment of the radar with regard to the maximum Doppler velocity, and slightly dependent on the drop-size distribution assumed.

The method is described for the adjustment of the Delft Atmospheric Research Radar (DARR), which was used for a verification experiment. This FM–CW type of radar is particularly suitable for the measurements because of its high sensitivity, range resolution and small sample processing bandwidth, but the method might also be used on high quality pulse radars.

2. Data acquisition

Measurements have been made for 120 S on 30 November 1981 during a prolonged stratiform rain of low intensity (0.4 mm h^{-1}). Under such circumstances mean vertical air velocities are expected to be very small; Ludlam (1980) gives a characteristic air velocity gradient of 0.02 m s^{-1} km^{-1} above the cloud base. Thus a bias in the observations can easily be determined.

The frequency modulated–continuous wave (FM–CW) radar, used in the verification experiment is described by Ligthart and Nieuwkerk (1980). Instrumental data are given in Table 1. The intensity of the reflection in the radar beam is recorded for several distance intervals to the radar (range cells) and several Doppler velocity intervals. Within each range cell the reflected power is distributed into velocity cells. As the fall velocity of the raindrops may reach 10 m s^{-1}, the Doppler velocity range is somewhat larger than the total velocity range.

TABLE 1. Instrumental data.

Radar wavelength	0.09 m
Beamwidth	1°
Range cell dimensions at 1 km	60 × 20 × 20 m
Velocity cell step	0.28 m s^{-1}
Maximum unambiguous velocity (V_{max})	9.03 m s^{-1}
Transmitted power	80 W
Minimum detectable reflectivity at 1 km	−28.4 dB(Z)
Reflectivity of rain R = 0.4 mm h^{-1}	+16.6 dB(Z)
Data repetition time in seconds	0.36 s

When the Doppler velocity exceeds the maximum unambiguous velocity, the FM–CW radar displays the reflectivity of a given range cell in the next range cell at a velocity that equals the difference between the Doppler and the maximum unambiguous velocity. Therefore in our situation the fastest falling drops of a given range cell will contribute to the succeeding range cell (see Fig. 1). At the same time some ambiguity is found for the lowest and highest velocity ranges because of the interaction between succeeding range cells, but actually this complicating effect is very useful in processing of the data. To get minimum influence of neighboring range cells, the boundary between two reflectivity profiles has to be selected at the point of minimal reflectivity.

We found considerable scatter in the location of points of minimal reflectivity between succeeding observations. The scatter is not attributable to instrumental noise which is at a level some 20 dB below the observed reflectivity at the boundaries. Ground clutter was observed in the first range cells only. As these cells were not used for further calculations, ground clutter cannot influence the results. The phase of the reflected radar wave is dependent on the distance of the reflective objects from the radar source. Then the reflected waves from different objects, resulting in different phases, will interact. A reasonable explanation of the observed scatter can be found in the interaction of reflected radar waves. In order to diminish the influence of interaction on the determination of the boundary location, the following processing techniques have been applied:

1) time averaging of successive observations;
2) smoothing of the reflectivity profiles around the minima; investigation showed that second order polynomials provided a satisfactory fit to the observations.

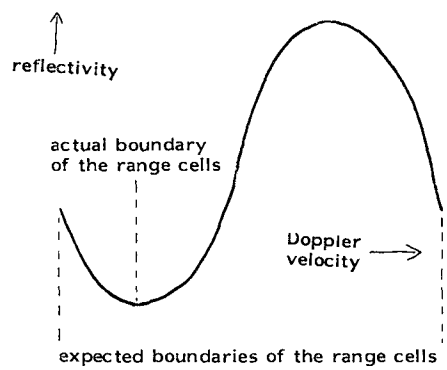

FIG. 1. The reflected power as a function of the Doppler fall velocity within a range cell. The high reflectivity on the left is caused by fast falling drops of the neighboring range cell.

3. Determination of the air velocity

With the boundary between succeeding reflectivity profiles, a quantity is determined that is related to the local vertical air velocity V_a. Therefore the significance of the velocity at which the boundary is set (called boundary velocity V_b) is analyzed. At the boundary velocity, small reflectivity values are expected for the slowest drops in the considered range cell and for the fastest drops of the previous one; the radar is insensitive to the smallest slow falling drops, and a low reflectivity value is measured for a few large and fast falling drops. So the boundary velocity indicates the boundary between the largest drops of a given range cell and the smallest drops of the preceding cell. In presence of vertical air velocities the fall velocities relative to the radar will change for all raindrops. Then also the boundary velocity will change. Therefore a relation is expected between air velocity and boundary velocity. Contrary to the Lower Bound Technique this method also uses the reflectivity of the fastest falling drops.

To find the relation between air and boundary velocity and to analyze what other quantities may influence the boundary velocity, the reflectivity profile is parameterized with the Marshall and Palmer (1948) exponential distribution:

$$N_D = N_0 \exp(-\lambda D), \tag{1}$$

where N is number of drops per unit volume, D drop diameter and $\lambda = 4.1 \times R^{-0.21}$ (mm^{-1}), and with the Rayleigh radar reflectivity factor Z,

$$Z_D = Z_0 N_D D^6, \tag{2}$$

and with the measurements of Gunn and Kinzer (1946) for the relation between drop diameter and fall velocity.

The reflectivity profile for R = 0.4 mm h^{-1} as a function of fall velocity is shown in Fig. 2a. Part of the reflectivity profile of the neighboring range cell is also shown. As explained in Section 2, the following profile is displayed with a shift equal to the maximum unambiguous velocity. As this velocity was set at 9.03 m s^{-1}, somewhat below the maximum fall velocity of raindrops, the profiles of succeeding range cells overlap and the boundary velocity is found at the intersection of both profiles. In fact the boundary

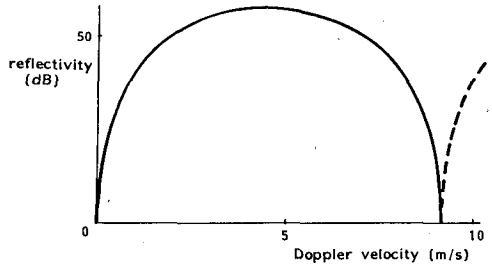

FIG. 2a. The calculated reflectivity as a function of fall velocity. The curve at the right represents the reflectivity of the neighboring range cell.

velocity should be calculated from the minimum of the best-fit second order polynomial. However, as can be seen from Fig. 2a, for $R = 0.4$ mm h^{-1} the profile is almost symmetrical and the minimum of the best-fit polynomial becomes equal to the intersection. For asymmetric profiles, which are found for high rainfall rates, the boundary velocity has to be calculated from the best-fit polynomial.

In the presence of a vertical air velocity V_a all fall velocities relative to the radar V_r will change with the same amount V_a; consequently the boundary velocity V_b will be shifted over V_a so that $(V_b - V_a)$, the difference between vertical air and boundary velocity, is independent of the air velocity. To find $(V_b - V_a)$ we analyzed what quantities may influence the boundary velocity at $V_a = 0$.

Unfortunately, the fall velocity measurements used in the calculations could not be expressed in a simple analytical expression for the range (of extremely small and extremely large drops) where the succeeding reflectivity profiles intersect. Therefore, the theoretical boundary velocity is calculated graphically from the reflectivity profile. Fig. 2b shows some calculated profiles near the intersection. It is seen that at low fall velocities the reflectivity profile is hardly influenced by rainfall rate or air density. This suggests that only the low fall velocity part should be used for the air velocity determination (Lower Boundary Technique). However, the Lower Boundary Technique will give ambiguity because of broadening of the reflectivity profile, as will be explained in Section 4.

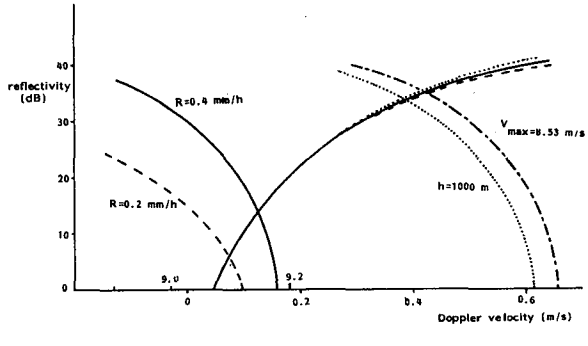

FIG. 2b. The calculated reflectivities as a function of fall velocity near the boundary between two succeeding range cells in several situations. The curves from the lower left to the upper right represent the low fall velocity part of the reflectivity profile; the other curves show the matching high fall velocity part of the neighboring range cell. Note the double scaling for the velocity in both range cells. The boundary velocity is found at the intersection of two matching curves of succeeding range cells.

Figure 2b shows the boundary velocity strongly dependent on the shift between succeeding range cells and, therefore, also on the maximum unambiguous velocity of the radar: $V_b = 0.12$ m s^{-1} for $V_{max} = 9.03$ m s^{-1} and $V_b = 0.43$ m s^{-1} for $V_{max} = 8.53$ m s^{-1}. For the most accurate results, it seems preferable to derive the relation between air and boundary velocity for every value actually used for the maximum unambiguous velocity of the radar. Therefore the derivation is restricted to $V_{max} = 9.03$ m s^{-1}, the value used in the measurements. Furthermore, Fig. 2b shows a strong dependence between boundary velocity and measuring height h. Because of decreasing air density with height the maximum fall velocity of raindrops increases almost 0.5 m s^{-1} km^{-1} above the earth surface (Beard *et al.*, 1976), resulting in a shift in the boundary velocity V_b of 0.3 m s^{-1} km^{-1}. Finally, Fig. 2b shows that rainfall rate will have only a minor influence on the calculated boundary velocity; doubling the rainfall rate will result in a shift of only 0.05 m s^{-1} on the boundary velocity. The calculations were made for several rainfall rates between 0.1 and 1 mm h^{-1}. In this range the logarithmic dependence between rainfall rate and boundary velocity $V_b = 0.17 \times \log R + 0.17$ for $V_z = 0$ and $h = 0$ was found to agree well with the calculations.

Accepting the Marshall and Palmer distribution, we could not find other quantities that influence the relation between boundary and vertical air velocity. As maximum unambiguous velocity of the radar and measuring height may be determined with high accuracy and with only a small influence of rainfall rate on boundary velocity, the boundary velocity seems to be well suited for the determination of vertical air velocity. For light rain and a maximum unambiguous velocity of 9.03 m s^{-1}, vertical air velocity is calculated:

$$V_a = V_b - 0.17 - 0.17 \log R - 0.0003h, \quad (3)$$

where h is measuring height in m above 1013 mb.

4. Turbulent vertical air velocity

Determination of the drop-size distribution requires knowledge of the fall velocity relative to the surrounding air. Therefore, we must measure Doppler fall velocity and air velocity V_a simultaneously. Owing to turbulence, the vertical air velocity will fluctuate within the space and time interval of the measurement. Fall velocity of raindrops is rapidly adapted to air velocity fluctuations; even the largest drops are

adapted within a fall of 20 m; so vertical air velocity fluctuations will result in fluctuations of the fall velocity relative to the radar V_r. Then drops of a certain diameter are displayed with different fall velocities V_r. This results in broadening of the reflectivity-fall velocity profile.

Broadening of the reflectivity profile may set severe limitations on the suitability of the Lower Boundary Technique. The influence on the boundary velocity, however, is only small as the broadening occurs for the smallest as well as the largest drops, giving compensary effects on the location of the boundary. A small space and time interval is required for measurements of drop-size distributions as broadening will result in over-estimation of the amount of the smallest and largest raindrops. However in small time and space intervals only a few raindrops are present. Then the interaction of reflected radar waves becomes more important and the boundary velocity can be determined with less accuracy. Hence, an optimal sampling space and time is expected for the determination of drop-size distributions. This optimum is found when the fluctuations in the vertical air velocity are measured most accurately. Therefore the influences of vertical air velocity fluctuations and measurement errors on the boundary velocity are analyzed by writing:

$$V_b = V_a + V_m, \tag{4}$$

$$V_r = V_a + V_f + V_n, \tag{5}$$

where V_m is the measurement error in V_b, the mean value of V_m is given in Eq. (3); V_n is the measurement error in V_r; $\overline{V_n} = 0$; V_f the fall velocity relative to the air and V_r the observed fall velocity relative to the radar (= Doppler velocity).

The magnitude of the measurement errors and the true fluctuations will be represented by their variance, noted as σ^2; the covariance between A and B will be noted as $\sigma(A, B)$. The variance of the measurement error $\sigma^2 V_m$ and air velocity fluctuations $\sigma^2 V_a$ are found from the variances of V_b, V_r and $V_b - V_r$; with Eqs. (4) and (5) we find:

$$\sigma^2 V_b = \sigma^2(V_a + V_m) = \sigma^2 V_a + \sigma^2 V_m, \tag{6}$$

$$\sigma^2 V_r = \sigma^2(V_a + V_f + V_n) = \sigma^2 V_a + \sigma^2 V_f + \sigma^2 V_n + 2\sigma(V_a, V_f), \tag{7}$$

$$\sigma^2(V_r + V_b) = \sigma^2(V_f + V_n - V_m),$$

or

$$\sigma^2 V_r + \sigma^2 V_b - 2\sigma(V_r, V_b) = \sigma^2 V_f + \sigma^2 V_n + \sigma^2 V_m. \tag{8}$$

In these equations we have assumed that the measurement errors are not correlated to the true air and fall velocity fluctuations. Air and fall velocity may be correlated, as rain mostly occurs in ascending air, while raindrops may cause sinking air by fall drag. But as these phenomena need long interaction times, they will be neglected for estimation of the high frequency measurement errors; hence

$$\sigma(V_a, V_f) = 0. \tag{9}$$

The scatter in the air velocity is then found by subtracting Eqs. (6) and (7) from (8)

$$\sigma^2 V_a = \sigma(V_b, V_r), \tag{10}$$

and we derive from the same equations:

$$\sigma^2 V_m = \sigma^2 V_b - \sigma(V_b, V_r), \tag{11}$$

$$\sigma^2 V_f + \sigma^2 V_n = \sigma^2 V_r - \sigma(V_b, V_r). \tag{12}$$

These equations give the accuracies that are feasible by using the following approaches, in order to estimate the actual air velocity:

1) By assumption of steady state conditions, the turbulent air velocity fluctuations $\sigma^2 V_a$ are neglected.

2) By calculation of the air velocity from the boundary velocity, a measurement error $\sigma^2 V_m$ is introduced.

3) By calculation of the air velocity from the Doppler fall velocity (Hauser and Amayenc, 1980) the high frequency fluctuations in the fall velocity $\sigma^2 V_f$ are neglected and a measurement error $\sigma^2 V_n$ is introduced.

5. Results

Data have been collected for two minutes as described in Section 2. The computed mean Doppler velocity and reflectivity are shown in Fig. 3. The bright band is found at 1.3 km height, while another band at 3.4 km marks the upper boundary of the cloud. The cloud base was below 250 m so that all rain measurements are within the cloud. The decreasing reflectivity with height in the rain can be explained by a decrease in rainfall rate. According to Marshall and Palmer (1948), we have the equation

$$Z = 200R^{1.6},$$

resulting in an exponential decrease from $R = 0.45$ mm h^{-1} at 0.3 km to $R = 0.34$ mm h^{-1} at 1.3 km height.

Mean air and fall velocities are shown in Fig. 4. Up to 1.1 km height, excellent agreement with the calculated values has been found. Even the small upward air velocity near the ground might be explained by the influence of the high building (90 m), on which the radar is mounted. The larger deviation above 1.1 km is probably caused by some large, partly melted snowflakes, resulting in deviations from the assumed Marshall and Palmer raindrop distribution (Passarelli, 1976).

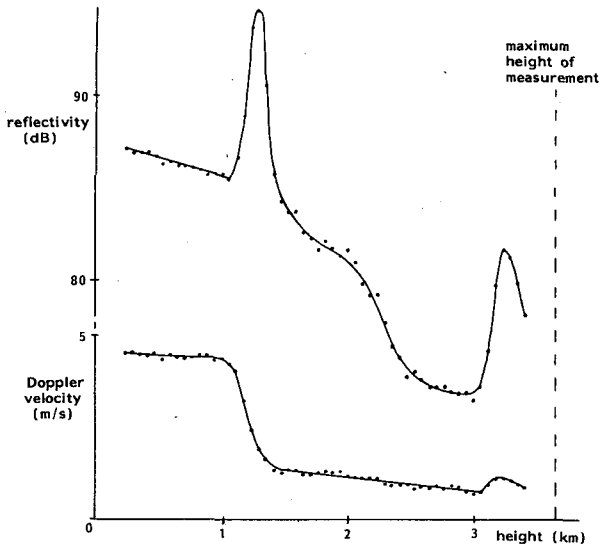

FIG. 3. Reflectivity and Doppler fall velocity as a function of height above the surface during the steady rain of 30 November 1981.

Deviations from the assumed raindrop distribution are mostly found at large drop sizes; improvements can be expected if the boundary velocity is calculated from the reflectivity of the smallest raindrops only. The scatter in the measurements is shown in Fig. 5. The scatter is defined here as the rms deviation of the actual value from the mean obtained from observations during a corresponding 23 s time interval. So, Fig. 5 gives only the high frequency fluctuations and Eq. 9 is still valid.

Fig. 5 shows that the lowest scatter, and therefore the highest accuracy, is obtained by calculating the air velocity from the boundary velocity. In this experiment the estimation of air velocity from the Doppler fall velocity gave accuracies comparable to the case, where the high frequency velocity fluctuations were neglected.

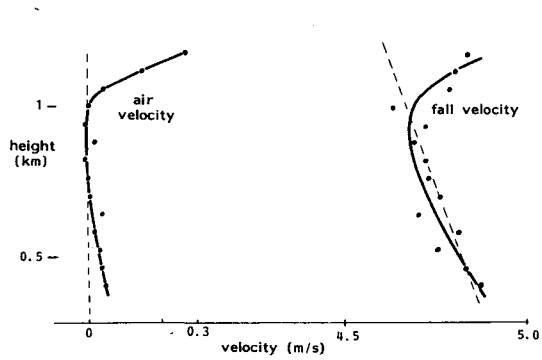

FIG. 4. Mean upward air velocity and downward fall velocity as a function of height on 30 November 1981. The dashed lines show the values calculated with Eq. (3); dots represent the observed values.

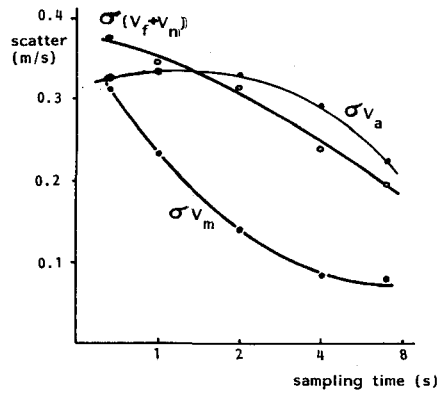

FIG. 5. The scatter in the air velocity (σV_a) compared to the measurement accuracy when the air velocity is calculated from the boundary velocity (σV_m), or from the fall velocity [$\sigma(V_f + V_n)$] as a function of sampling time.

The results of Fig. 5 are shown for several values of the sampling averaging time to find the optimal sampling time for the determination of air velocity fluctuations. For short sampling times the measurement accuracy decreases, while for long sampling times the air velocity fluctuations are followed less accurate. The optimal sampling time is found for the maximum difference between air velocity fluctuations and measurement errors. From Fig. 5 we find

1) Optimal sampling time = 3 s,
2) Measurement error $\sigma V_m = 0.11$ m s^{-1}.

Finally, Fig. 5 shows that air velocity fluctuations are constant for sampling times shorter than 3 s. It must be kept in mind that Fig. 5 does not give the Fourier transformed turbulence spectra, but the rms deviations from the mean value. This means that we do not measure any air velocity fluctuations for sampling times shorter than 3 s. Higher frequeny fluctuations may well be present in the atmosphere, but are damped out in the observations, due to the dimensions of the scan volume. With a maximum scan volume dimension of 60 m and a horizontal wind velocity of 18 m s^{-1}, a frequency cut-off is expected at 18/60 = 0.3 Hz, which is in agreement with the observations. Combining this result with the extremely low measurement errors we may expect that the high frequency air velocity fluctuations can be followed even more accurately by reducing the scan volume.

6. Evaluation

The mean air velocity is determined very accurately from the reflectivity minimum, although some bias is to be found near the bright band. This is attributable to partly melted snowflakes, which cause deviations from the assumed reflectivity profile.

Model calculations show that most deviations are

expected at high fall velocities. So in situations of uncertain drop-size distributions mean air velocity might be determined with less ambiguity by using the reflectivity profile of the low fall velocities only. But when rain is falling through unsaturated air the reflectivity profile of the fastest falling drops is expected to give the most accurate results as the smallest drops might be evaporated. Therefore, it is recommended that the situation be analyzed before choosing the method of data processing. The influence of interaction between reflected radar waves is reduced by fitting a curve to the observed reflectivity profile. In consideration of the extremely low scatter in the results ($\sigma V_m = 0.11$ m s^{-1}), this technique works very well. The resulting scatter is well beyond the accuracy of 0.25 m s^{-1} required for the determination of raindrop spectra. Whether the technique of curve-fitting on the low fall velocity reflectivity profile only will give a comparable low scatter will depend on the feasibility of representing this part of the reflectivity profile with a useful curve.

The curve-fitting technique around the reflectivity minimum has given considerably less scatter than estimation of the actual air velocity from its mean value or from the actual fall velocity. This suggests that the boundary velocity is less influenced by fluctuations of the drop-size distribution than the mean fall velocity. Further, this result is explained by steepness of the reflectivity profile near the boundary velocity so that the boundary velocity is rather insensitive to deviating reflectivity profiles. It is probable that these differences will be even more pronounced in situations of higher turbulence since the scatter in this method results mainly from wave interaction rather than atmospheric conditions. Therefore, the method seems to be particularly suitable for use in turbulent precipitation.

The method might be used for real-time data processing since all variables that determine the mean value and fluctuations in the air velocity are known or measured. It seems that the most accurate determination of rainfall rate for use in Eq. (3) comes from the actual total reflectivity in the range cell concerned, but the fluctuations in the total reflectivity are not yet completely understood. Therefore the rainfall rate has been assumed to be constant in time and dependent only on height. Only one variable, the sampling time, must be estimated from previous measurements.

Acknowledgments. The author wishes to express his thanks especially to Dr. Ligthart and Dr. Nieuwkerk for use of the radar and for assistance in data interpretation; and to Dr. van der Hage for exchange of ideas on meteorological applications.

REFERENCES

Atlas, D., R. C. Srivastava and R. S. Sekhon, 1973: Doppler-radar characteristics of precipitation at vertical incidence. *Rev. Geophys. Space Phys.*, **2**, 1–35.

Beard, K. V., 1976: Terminal velocity and shape of cloud and precipitation drops aloft. *J. Atmos. Sci.*, **33**, 851–864.

Gunn, R., and G. D. Kinzer, 1949: The terminal velocity of fall for water droplets in stagnant air. *J. Meteor.*, **6**, 243–248.

Hauser, D., and P. Amayenc, 1980: A new method for deducing hydrometeor size distributions and vertical air motions from Doppler Radar measurements at vertical incidence. *Preprints 19th Radar Meteor. Conf.* Miami, Amer. Meteor. Soc.

Ligthart, L. P., and L. R. Nieuwkerk, 1980: F.M.-C.W. Delft atmospheric research radar. *Proc. IEEE*, **127**, 421–426.

Ludlam, F. H., 1980: *Clouds and Storms.* Pennsylvania State University Press, 353 pp.

Marshall, J. S., and W. McK. Palmer, 1948: The distribution of raindrops with size. *J. Meteor.*, **5**, 165–166.

Passarelli, R. E., 1976: Coordinated Doppler radar and aircraft observations of riming and drop breakup in stratiform precipitation. *Proc. Int. Conf. on Cloud Physics*, 500–505.